Survival of the magnetotactic bacterium *Magnetospirillum gryphiswaldense* exposed to Earth's lower near space

Jia Liu[1,2,3], Wensi Zhang[1,3], Kuang He[1,3,4], Li Liu[1,3,5], Chao Wang[6], Yuanda Jiang[6], Shijiao Ma[3,7], Jiesheng Tian[3,7], Ying Li[3,7], Tongwei Zhang[1,3], Lanxiang Tian[1,3], Fei He[1], Greig A. Paterson[8], Yong Wei[1,5], Yongxin Pan[1,3,5], Wei Lin[1,3]*

[1]Key Laboratory of Earth and Planetary Physics, Institute of Geology and Geophysics, Chinese Academy of Sciences, Beijing 100029, China;

[2]CAS Key Laboratory of Marine Ecology and Environmental Sciences, Institute of Oceanology, Chinese Academy of Sciences, Qingdao 266071, China;

[3]France-China Joint Laboratory for Evolution and Development of Magnetotactic Multicellular Organisms, Chinese Academy of Sciences, Beijing 100029, China;

[4]Frontiers Science Center for Deep Ocean Multispheres and Earth System, Key Lab of Submarine Geosciences and Prospecting Techniques, MOE and College of Marine Geosciences, Ocean University of China, Qingdao 266100, China

[5]College of Earth and Planetary Sciences, University of Chinese Academy of Sciences, Beijing 100049, China

[6]Key Laboratory of Electronics and Information Technology for Space Systems, National Space Science Center, Chinese Academy of Sciences, Beijing 100190, China;

[7]State Key Laboratories for Agro-biotechnology and College of Biological Sciences, China Agricultural University, Beijing 100193, China.

[8]Department of Earth, Ocean and Ecological Sciences, University of Liverpool, L69 7ZE, Liverpool, UK.

***Corresponding author.**

E-mail: weilin@mail.iggcas.ac.cn

Earth's near space (20-100 km above sea level) is one of the most extreme environments on Earth due to a combination of high radiation, low atmospheric pressure, extreme cold and hyper aridity [1]. Investigations of the survival strategies of microorganisms in near space are of great interest in respect of understanding the limits of life on Earth, identifying the upper boundary of Earth's biosphere, testing the panspermia hypothesis, and assessing long-distance microbial transfer [2]. High-altitude balloon based research on microorganisms in near space dates back to the 1930's [3]. Ultraviolet (UV) radiation has been shown to be one of the main causes of biological mortality in near space. Thus to date many extremophilic microorganisms including bacteria, archaea and fungi have been tested for their tolerance to extreme conditions in the stratosphere region of lower near space [4].

Magnetotactic bacteria (MTB) are a group of microorganisms able to passively align along geomagnetic field lines and are characterized by their ability to synthesize intracellularly magnetic organelles (known as magnetosomes) consisting of lipid bilayer-bounded membranes, in which nanosized, ferrimagnetic magnetite (Fe_3O_4) and/or greigite (Fe_3S_4) crystals are biomineralized [5]. Magnetoreception is the major function of magnetosomes in modern MTB, while Fe_3O_4-type magnetosomes have been revealed to play an enzyme-like role to eliminate intracellular levels of toxic reactive oxygen species (ROS) in *Magnetospirillum gryphiswaldense* strain MSR-1 (MSR-1) [6], indicating the potential of MTB to tolerate high levels of UV radiation. Moreover, MTB are considered to be one of the earliest magnetic-sensing organisms that emerged in the Archean Eon when Earth lacked a stable thick ozone layer and was exposed to extremely high fluxes of UV radiation [7]. Therefore, studying the tolerance of MTB under high UV doses will lead to a better understanding of the origin and early evolution of MTB. Previously, UVB radiation (peaking at 306 nm) has been revealed to affect the cell growth and magnetosome formation in *M. magneticum* strain AMB-1 (AMB-1) under laboratory conditions [8]. However, our understanding of the effects of natural solar UV radiation on MTB remains very limited.

Here, we performed experimental exposure of wildtype and magnetosome-deficient MSR-1 strains (Fig. S1 and the Supplementary materials for strain description and culture condition) to Earth's lower near space at ~23 km above sea level (ASL) through a high-altitude scientific balloon using the Chinese Academy of Sciences Balloon-Borne Astrobiology Platform (CAS-BAP) during the HH-20-7 flight mission [9]. Samples of MSR-1 were freeze-dried beforehand to reduce damage from freeze-thawing processes during the flight (Fig. 1a and the Supplementary materials for sample preparation and experimental design). The BIOlogical Samples Exposure Payload (BIOSEP) is a box-shaped vessel that accommodates biological/chemical samples in a 30-cell (61 mm in diameter, Fig. S2) sample chamber and four 96-well plates (Fig. 1b). The BIOSEP was mounted at an elevation angle of 30° relative to the

horizon, and hence the normal of the windows of the sample chambers is 60° above the horizon. Chamber cells were kept sealed from the outside environment to maintain a constant internal pressure and humidity. The BIOSEP was launched at 01:02 China Standard Time (CST) on September 3, 2020 into the lower near space at Dachaidan, Qinghai, China (37°44′ N, 95°21′ E) and flew for a total of 18 hours and 44 minutes using a 50,000 m^3 high-altitude helium balloon. The payload stayed at a floating altitude of 23 km for 14 hours (Fig. 1c). Samples were remained shielded inside the BIOSEP until 07:59 CST, at which point the flight computer remotely lifted the box lid of BIOSEP to start the exposure experiments. The box lid was closed at 15:15 CST after 7 hours and 16 minutes of exposure, with a period of direct exposure for 5 hours 18 minutes as monitored by illumination measurements (Fig. 1d and the Supplementary materials for data analysis). The level of diffuse UV radiation (191-399 nm) was measured by the UltraViolet Spectrometer (UVS) next to the BIOSEP. The diffuse UV radiation dose received by samples during the direct exposure was ~2.42×10^4 J/m^2 (Fig. 1e and the Supplementary materials for UV radiation measurement). According to the MODerate resolution atmospheric TRANsmission (MODTRAN) model [10], the direct solar UV spectrum at an altitude of 23 km near Dachaidan is approximately two orders of magnitude higher than the diffuse radiation spectrum (Fig. 1f). Moreover, in situ temperature in the sample chamber cell was monitored, which gradually increased from -43.9 to 33.8°C with the duration of continuous exposure (Fig. 1d). All samples were successfully recovered and stored in an automotive refrigerator at 4°C within 5 hours of landing. The laboratory control group (LCG) of freeze-dried MSR-1 was remained in a light-free refrigerator at 4°C in the laboratory (Fig. 1a).

After the flight, the number of surviving MSR-1 in each sample was estimated by colony-forming unit (CFU) enumeration. For the near space non-exposed group (NNG, launched to the near space but shielded by an opaque lid), CFU estimates of MSR-1 capable of magnetosome synthesis (referred to as MSR-1(+)) did not change significantly as compared to those of the LCG control group: the CFU estimates of NNG were $(2.21 \pm 0.15) \times 10^6$ CFU per chamber cell, and those of LCG were $(2.03 \pm 0.12) \times 10^6$ CFU per chamber cell (Fig. 2a and Table S1). In contrast, the survival rates of the near-space exposed group (NEG) decreased significantly ($F = 51.5$, $P < 0.001$), and culturable MSR-1(+) of NEG dropped by an order of magnitude to $(2.50 \pm 0.22) \times 10^5$ CFU per chamber cell. For samples that did not form intracellular magnetosomes (referred to as MSR-1(-)), exposed bacteria suffered more significant inactivation after flight (Fig. 2a and Table S1). In contrast to MSR-1(+) that retained ~12.32% of viable cells after exposure, no culturable colonies of MSR-1(-) were observed in all NEG samples. Moreover, a considerable degree of inactivation of the NNG MSR-1(-) samples was also noted; that is, only ~27.97% of bacteria survived even without UV radiation exposure. The different viability

between exposed MSR-1(+) and MSR-1(-) indicates that magnetosomes may play an important role in protecting MTB from UV irradiation.

To investigate the effects of near-space exposure on magnetosome formation, we examined the variations in the number and crystal size of magnetosome of surviving MSR-1(+) using transmission electron microscopy (TEM). MSR-1 with intracellular magnetosomes accounted for 95.6% of the total surviving cells in NEG, while only 84.5% of cells in LCG were capable of synthesizing magnetosomes, suggesting that cells with magnetosomes are more likely to survive after near-space exposure. Magnetite crystals within each single MSR-1 cell formed one magnetosome chain (Fig. 2b), with average crystal numbers of 16.0 ± 5.4 in NEG and 14.8 ± 6.0 in LCG (Fig. 2c). For NEG, cells that synthesize more than 10 magnetosomal crystals accounted for 90.3% of the total cells (n = 134); however, this proportion in LCG dropped to 75.7% (n = 112) (Fig. 2c). There were 86.6% of magnetosomes with grain sizes of 25-55 nm in NEG (n = 822), while this proportion decreased to 81.5% in LCG (n = 800) (Fig. 2d). Magnetosomal crystals less than 25 nm accounted for 8.3% and 11.5% in the NEG and LCG samples, respectively; and those larger than 55 nm accounted for 5.1% and 7.0% in the NEG and LCG samples, respectively.

Rock magnetic measurements were performed to characterize the bulk magnetic properties of MSR-1(+) samples. The room-temperature hysteresis loops of both NEG and LCG yield pot-bellied shapes. The reproducibility of the parallel samples in LCG was better than those in NEG (Fig. 2e). The values of coercivity of remanence (B_{cr}) for NEG and LCG ranged from 26.0 to 31.0 mT and 27.9 to 29.6 mT, respectively. The first-order reversal curve (FORC) diagrams of NEG and LCG have the typical characteristics of noninteracting uniaxial single domain particles, indicating that the bulk samples retain intact chains as shown in Fig. 2f. Low-temperature magnetization curves revealed that the δ_{FC}/δ_{ZFC} ratios of NEG and LCG were 3.4 and 2.8, respectively. Carter-Stiglitz et al. (2002) showed that the value of δ_{FC}/δ_{ZFC} ratios increased from 1.97 ± 0.32 to 2.28 ± 0.52 when the magnetosome number increased from 5 to 10 in one chain [11]. For our magnetic results, δ_{FC}/δ_{ZFC} ratio of NEG is larger than that of LCG, indicating that NEG has more magnetosomes per chain than the LCG. Together with TEM observations, these results suggest that MSR-1 with more magnetosomes may have a better chance to survive after near space flight exposure. Alternatively, extreme environmental conditions during flight (e.g., high UV radiation and temperature variation) may affect the synthesis of magnetosomes in MTB.

In a previous study, Wang et al. showed that living cells of AMB-1 exposed to UVB radiation (peaking at 306 nm) with a maximum dose of 1800 J/m^2 could affect the cell growth and magnetosome formation, resulting in more and larger magnetosomes per cell [8]. Our study

reveals that a fraction of freeze-dried MSR-1 with magnetosomes are able to survive in near space conditions with direct UV radiation of ~10^6 J/m^2 dose (wavelength recorded from 191 to 399 nm). The surviving cells after exposure synthesize larger numbers of and more uniformly sized magnetosomes. Previously, organisms used for near-space exposure experiments were normally extremophiles and spores [4, 12], and most of them are found to suffer from a significant loss of viability under such high levels of UV radiation (with survivability of 0-50% under ≥2 hours of exposure at 20-40 km ASL) [4, 12, 13, 14 and references herein]. The results of our work are noteworthy because MSR-1 is not an extremophile – it was isolated from a normal aquatic environment and does not produce spores. The finding that after near space exposure MSR-1(+) remain viable while MSR-1(-) are completely inactivated in this study, together with previous studies [6], indicates that magnetosomes very likely play an important role in protecting MTB from UV radiation. Although the underlying mechanisms of the magnetosome-mediated UV defense are not fully understood yet, the peroxidase-like activity of magnetite crystals is thought to be one possibility. UV-induced ROS could damage important cellular components such as peptide chain fragmentation, enzyme inactivation, lipid peroxidation and DNA oxidative damage [15]. Magnetosomes in MSR-1 have been shown to exhibit peroxidase-like activity that could eliminate intracellular levels of ROS [6]. Therefore, magnetosomes may act as antioxidative compounds to protect MSR-1 from UV damage. Another possible mechanism is the optical screening of UV wavelengths by magnetosomes. Some bacteria and yeasts accumulate pigments to absorb a range of light spectrum. MTB invest a great deal of energy to synthesize magnetosomes which enable the accumulation of intracellular magnetite, resulting in colonies dark brown in color. Visual inspection of the exposed samples revealed slightly alterations in color that indicates a potential photochemical process mediated by magnetosomes that may serve to reduce the UV dose or deplete irradiation energy. The third mechanism is that the lower layers of MSR-1 may be physically protected from UV by upper layers of bacterial cells and their magnetosome chains. The number of bacterial layers in this study was estimated to be about five, and the UV transmittance regarding the number of layers are shown in Table S2.

One limitation of this study is the use of freeze-dried cells that are not metabolically active. A temperature control system that can better reflect the metabolic and physiological changes of active bacterial cultures is crucial for future research. Moreover, laboratory-based simulation chambers with fully controllable environmental conditions are also important in future studies and should attempt to focus broad spectrum UV radiation rather than a single wavelength. Considering that Earth's lower near space is an exemplary analog to the present-day Martian surface and the atmosphere of Venus [2, 12], the survivability of MTB in this region suggests that MTB can be valuable candidates for astrobiology research. Further studies on MTB

exposure, not only to near space but also to the environments around space stations (e.g., the China's Space Station and the International Space Station) should be highly anticipated.

Conflict of interest

The authors declare that they have no conflict of interest.

Acknowledgments

The authors would like to thank all people involved with the Scientific Experimental System in Near Space (SENSE) Project of HH-20-7 flight mission. We thank Taihua Zhang for providing the flight data. We thank Yingjie Li, Qing Liu, Runjia Ji and Tian Xiao for useful discussion. This work was supported by the Strategic Priority Research Program of Chinese Academy of Sciences (XDA17010501), the National Natural Science Foundation of China (NSFC) grants 41822704 and 41621004, the Youth Innovation Promotion Association of the Chinese Academy of Sciences, and the Key Research Programs of the Institute of Geology and Geophysics, Chinese Academy of Sciences (IGGCAS-201904 and IGGCAS-202102). Greig A. Paterson is support by a Natural Environment Research Council (NERC) Independent Research Fellowship (NE/P017266/1).

Author contributions

Wei Lin and Jia Liu conceived the project, designed the experiments, interpreted the results and wrote the manuscript with contributions from all authors. Jia Liu, Wensi Zhang, Kuang He and Li Liu performed the culture experiments, sample preparation, TEM observation, cell activation, rock magnetic experiments and data analysis. Chao Wang and Yuanda Jiang performed the environmental data experiments including pre-experiments using BIOSEP. Fei He provided UV data and contributed to the analysis. Shijiao Ma, Jiesheng Tian and Ying Li assisted with the culture experiments of MSR-1. Greig A. Paterson, Tongwei Zhang, Lanxiang Tian, Yong Wei and Yongxin Pan contributed to data interpretation and manuscript proofreading. All authors read and approved the final manuscript.

References

[1] Young M, Keith S, Pancotti A. An overview of advanced concepts for near space systems. in 45th AIAA/ASME/SAE/ASEE Joint Propulsion Conference & Exhibit, Denver, Colorado, 2 to 5 August 2009. doi: 10.2514/6.2009-4805.

[2] Smith DJ, Sowa M. Ballooning for biologists: mission essentials for flying life science experiments to near space on NASA large scientific balloons. Gravit Space Res 2017; 5: 52-73.
[3] Rogers LA, Meier FC. The collection of microorganisms above 36,000 feet. Nat Geo Soc Stratos Ser 1936; 2: 146–151.
[4] DasSarma P, DasSarma S. Survival of microbes in Earth's stratosphere. Curr Opin Microbiol 2018; 43: 24-30.
[5] Uebe R, Schüler D. Magnetosome biogenesis in magnetotactic bacteria. Nat Rev Microbiol 2016; 14: 621-637.
[6] Guo FF, Yang W, Jiang W, et al. Magnetosomes eliminate intracellular reactive oxygen species in *Magnetospirillum gryphiswaldense* MSR-1. Environ Microbiol 2012; 14: 1722-1729.
[7] Lin W, Paterson GA, Zhu Q, et al. Origin of microbial biomineralization and magnetotaxis during the Archean. Proc Natl Acad Sci U S A 2017; 114: 2171-2176.
[8] Wang Y, Lin W, Li J, et al. Changes of cell growth and magnetosome biomineralization in *Magnetospirillum magneticum* AMB-1 after ultraviolet-B irradiation. Front Microbiol 2013; 4: 397.
[9] Lin W, He F, Zhang W, et al. Astrobiology at altitude in Earth's near space. Nat Astron 2022; 6: 289.
[10] Berk A, Conforti P, Kennett R, et al. MODTRAN6: a major upgrade of the MODTRAN radiative transfer code. 2014 6th Workshop on Hyperspectral Image and Signal Processing: Evolution in Remote Sensing (WHISPERS) 2014; 90880H.
[11] Carter-Stiglitz B, Jackson M, Moskowitz B. Low-temperature remanence in stable single domain magnetite. Geophys Res Lett 2002; 29: 1129.
[12] Smith DJ. Microbes in the upper atmosphere and unique opportunities for astrobiology research. Astrobiology 2013; 13: 981-990.
[13] Pulschen AA, de Araujo GG, de Carvalho ACSR, et al. Survival of extremophilic yeasts in the stratospheric environment during balloon flights and in laboratory simulations. Appl Environ Microbiol 2018; 84: e01942-01918.
[14] Cortesão M, Siems K, Koch S, et al. MARSBOx: fungal and bacterial endurance from a balloon-flown analog mission in the stratosphere. Front Microbiol 2021; 12: 601713.
[15] Gao Q, Garcia-Pichel F. Microbial ultraviolet sunscreens. Nat Rev Microbiol 2011; 9: 791-802.

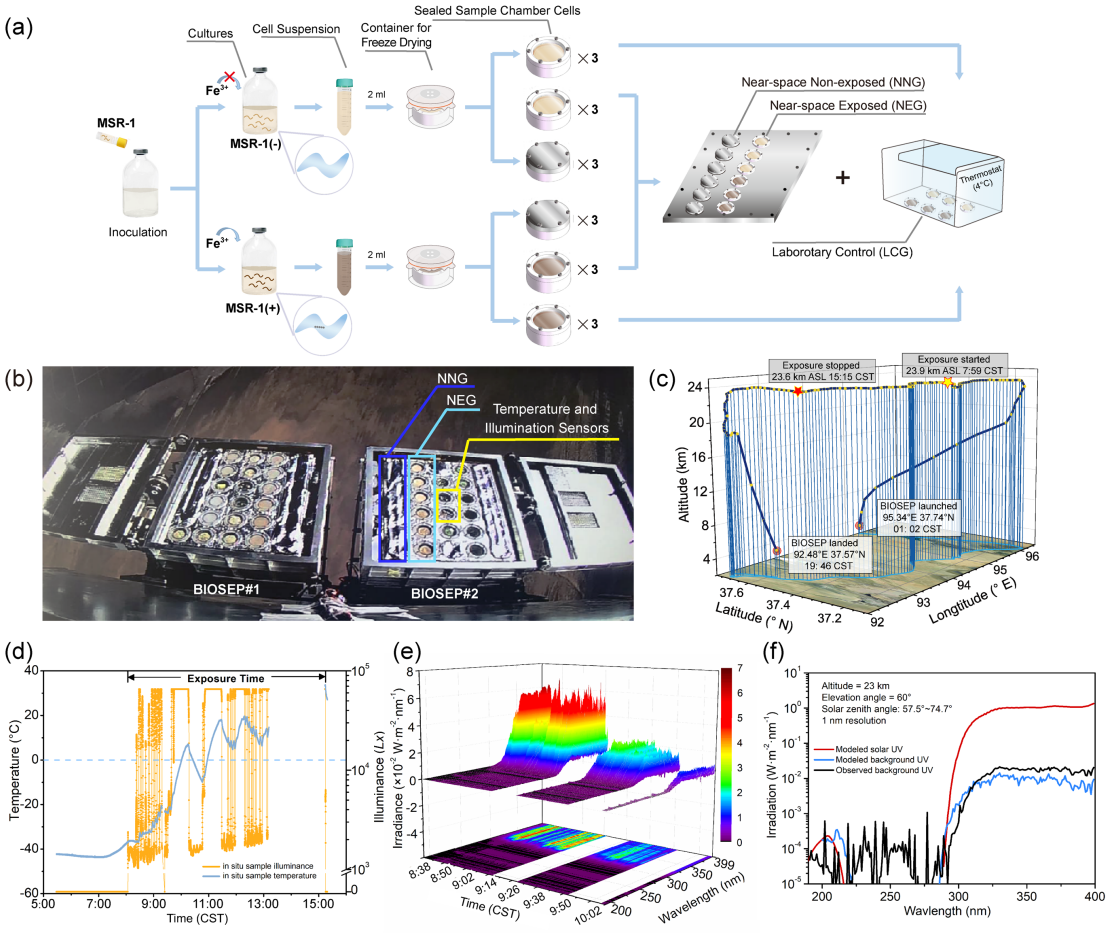

Figure 1. Near-space exposure experiments of *Magnetospirillum gryphiswaldense* strain MSR-1 (MSR-1). (**a**) Scheme of sample preparation process. Culture medium with or without ferric citrate was used to obtain bacterial samples with (MSR-1(+)) and without (MSR-1(-)) magnetosomes. Sample chamber cells were divided into three groups: near-space exposed group (NEG), near-space shielded non-exposed group (NNG) and laboratory control group (LCG), each containing triplicate samples. (**b**) Image of two BIOlogical Samples Exposure Payloads (BIOSEP) at ~23 km in the lower near space. The chamber cells containing MTB samples are placed in the first (NNG) and second (NEG) columns from left to right in BIOSEP#2. (**c**) Travel map of the HH-20-7 flight mission. (**d**) Temperature and solar illumination measured by sensors parallel to the samples for inferring the direct and effective exposure time. The low-illumination regions represent the BIOSEP with its back to the Sun where the UV radiation for samples is negligible. Temperature gradually increases with the duration of continuous exposure. The temperature and solar illumination recording were interrupted during 13:11-15:14 CST. (**e**) Diffuse UV data recorded by UltraViolet Spectrometer (UVS). The wavelength recorded ranged from 191 to 399 nm with a spectral resolution of 1 nm. It should be noted that the UVS had a relatively small field of view and was mounted at a fixed pitch angle of 30° to monitor the diffuse UV radiation rather than the direct solar UV radiation. (**f**) The MODerate resolution atmospheric TRANsmission (MODTRAN) model show that the modeled diffuse radiation spectrum (blue line) is generally in consistent with the observation (black line), and the modeled direct solar UV spectrum (red curve) is approximately two orders of magnitude higher, mostly contributed from the significant enhancement in UVA.

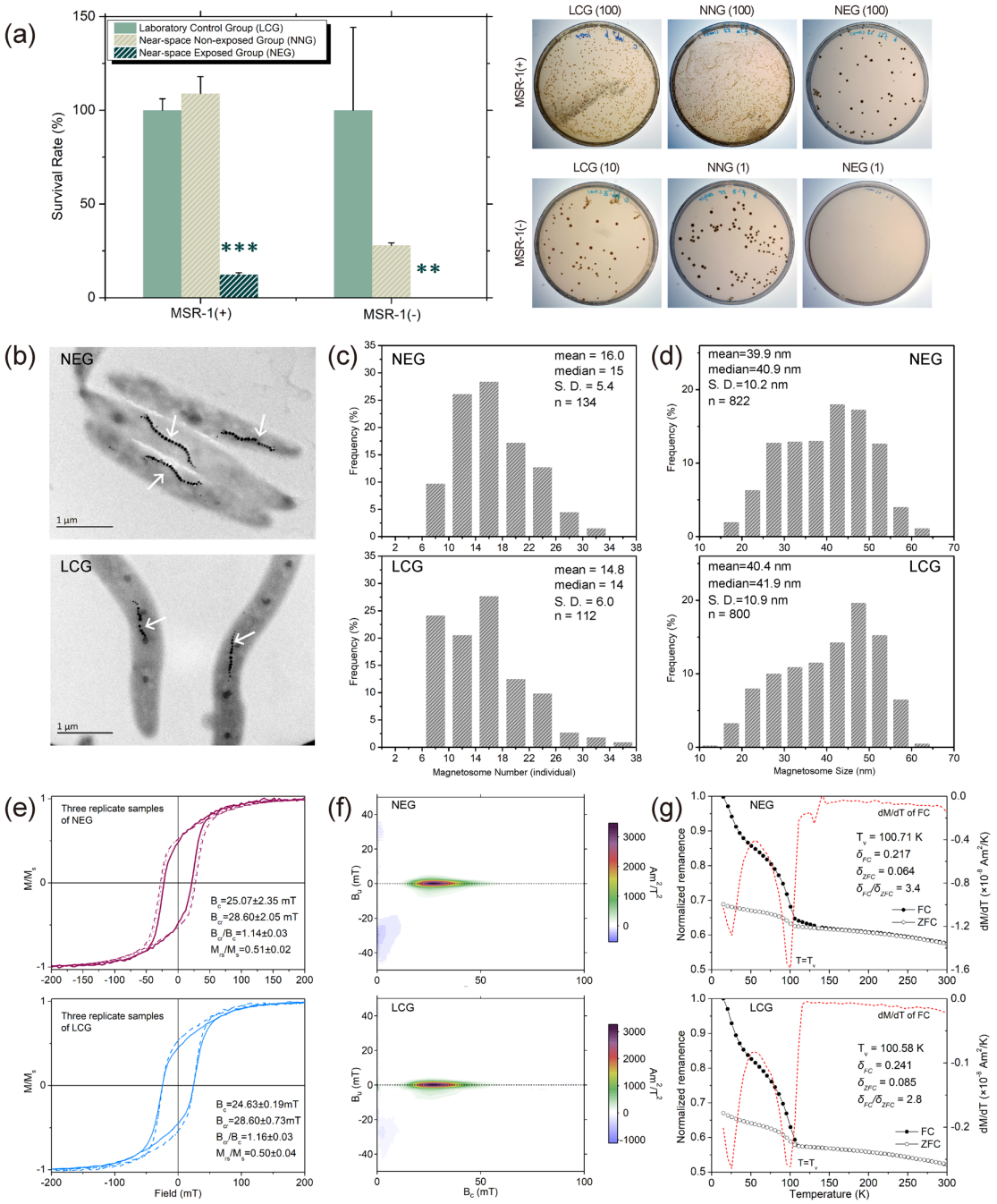

Figure 2. Survival rates, magnetosome features and rock magnetic properties of *M. gryphiswaldense* MSR-1. (**a**) Left: the freeze-dried cells of MSR-1 with magnetosomes (MSR-1(+)) gain a survival rate of ~12.32% after near space exposure while cells without magnetosomes (MSR-1(-)) are completely inactivated after exposure. Survival rates were determined as C_i / C_c, where C_i is the CFU in respective experimental groups and C_c is the CFU in the laboratory controls. The error bars represent the standard deviation of three duplicates. ** / *** Significant changes in survival rates with $P < 0.005$ / $P < 0.001$ (Table S1). Right: representative plates for counting colony forming units (CFU) of MSR-1. Numbers in parentheses represent the sample dilution folds. (**b**) Transmission electron microscope images of NEG and LCG MSR-1. White arrows indicate magnetosomes. (**c**) Histograms of magnetosome number per cell of NEG and LCG MSR-1. S.D. represents the standard deviation. (**d**) Histograms of magnetosomal crystal size of the two groups. (**e**) Room-temperature hysteresis loops of each group are normalized by the value of saturation magnetization (M_s). (**f**) First-order reversal curve (FORC) diagrams of the representative samples of the two groups. (**g**) Low-temperature magnetic measurements of the representative samples of the two groups.

Supplementary materials

Survival of the magnetotactic bacterium *Magnetospirillum gryphiswaldense* exposed to Earth's lower near space

Jia Liu[1,2,3], Wensi Zhang[1,3], Kuang He[1,3,4], Li Liu[1,3,5], Chao Wang[6], Yuanda Jiang[6], Shijiao Ma[3,7], Jiesheng Tian[3,7], Ying Li[3,7], Tongwei Zhang[1,3], Lanxiang Tian[1,3], Fei He[1], Greig A. Paterson[8], Yong Wei[1,5], Yongxin Pan[1,3,5], Wei Lin[1,3]*

[1]Key Laboratory of Earth and Planetary Physics, Institute of Geology and Geophysics, Chinese Academy of Sciences, Beijing 100029, China;

[2]CAS Key Laboratory of Marine Ecology and Environmental Sciences, Institute of Oceanology, Chinese Academy of Sciences, Qingdao 266071, China;

[3]France-China Joint Laboratory for Evolution and Development of Magnetotactic Multicellular Organisms, Chinese Academy of Sciences, Beijing 100029, China;

[4]Frontiers Science Center for Deep Ocean Multispheres and Earth System, Key Lab of Submarine Geosciences and Prospecting Techniques, MOE and College of Marine Geosciences, Ocean University of China, Qingdao 266100, China

[5]College of Earth and Planetary Sciences, University of Chinese Academy of Sciences, Beijing 100049, China

[6]Key Laboratory of Electronics and Information Technology for Space Systems, National Space Science Center, Chinese Academy of Sciences, Beijing 100190, China;

[7]State Key Laboratories for Agro-biotechnology and College of Biological Sciences, China Agricultural University, Beijing 100193, China.

[8]Department of Earth, Ocean and Ecological Sciences, University of Liverpool, L69 7ZE, Liverpool, UK.

***Corresponding author.**

E-mail: weilin@mail.iggcas.ac.cn

Materials and methods

Strain description and culture condition

Magnetospirillum gryphiswaldense strain MSR-1 (MSR-1), originally isolated from a eutrophic river nearby Greifswald, Germany, is one of the cultivable representatives of MTB [1]. The culture medium LA2 for MSR-1 was modified according to [2, 3] to achieve both high yields of bacterial cells and magnetosomes. The LA2 medium was made with (per liter of deionized water) 2 ml sodium L-lactate 60% solution, 0.34 g $NaNO_3$, 0.1 g KH_2PO_4, 0.15 g $MgSO_4 \cdot 7H_2O$, 2.38 g HEPES, 0.1 g yeast extract, 3 g soy bean peptone, 0.05 g sodium thioglycolate, 0.5 ml mineral elixir [3] and 60 μM ferric citrate. MSR-1 was incubated in flasks sealed with sand-cored silicone stoppers for 24 hours at 30°C (shaking at 100 rpm). MSR-1 incubated in this condition were used as the strain MSR-1(+) with intracellular magnetosomes. In addition, the ferric citrate-free LA2 medium was used to incubate MSR-1 cells without magnetosomes (MSR-1(-)).

Sample preparation

Prior to boarding the payload, MSR-1 were freeze-dried to reduce damage from the freeze-thaw process during flight. The cultures were firstly centrifuged at 3000 g for 5 min to remove the supernatant. Next, the remaining pellet was resuspended with a lyophilization protectant (5% trehalose solution), and 2-ml aliquots of bacterial suspensions were transferred to sterilized sample chamber cells within the vented sealing film-packed glass containers. Finally, after being pre-frozen at -80°C for 10 hours, MSR-1 samples were freeze-dried in vacuum using an Alpha 1-4 LSC plus Christ lyophilizer (Christ, Germany). All these operations were carried out under strictly sterile conditions.

Experimental design

For the exposure experiment, both MSR-1(+) and MSR-1(-) were divided into three groups: the near-space exposed group (NEG), the near-space non-exposed group (NNG) and the laboratory control group (LCG). Each group contained three replicates (Fig. 1a). Chamber cells

were sealed from the outside environment with constant pressure to remove the effects of pressure and desiccation. Both the NEG and NNG samples were launched into near space with the BIOlogical Samples Exposure Payload (BIOSEP): NEG were exposed to solar radiations through UV-grade quartz glass (Tangsinuo, China) that enabled >85% transmission of UV at 200 nm and >91% transmission of UV at 210-280 nm, while NNG were shielded from solar radiations by opaque aluminum lids (Fig. S2). As the control, LCG were stored at 4°C in the laboratory. All these samples were prepared from the same batch.

UV radiation measurement

The strength of UV (191-399 nm) radiation at the float altitude was measured by the UltraViolet Spectrometer (UVS, with a temporal resolution of 3 seconds). With a relatively small field of view, UVS was mounted at a fixed pitch angle of 30° to monitor the diffuse UV radiation instead of the direct solar UV radiation. The data acquisition had lasted for 1 hours and 30 minutes. The diffuse radiation dose was 2.86 J/m^2 for vacuum ultraviolet (VUV, 191-200 nm), 47.16 J/m^2 for UVC (200-280 nm), 588.53 J/m^2 for UVB (280-320 nm) and 6213.88 J/m^2 for UVA (320-400 nm). Considering the transmission efficiency (>85% for VUV and >91% for UVC) of the UV-grade quartz glass of each sample chamber cell, the diffuse doses of VUV and UVC received by MTB samples were 2.43 J/m^2 and 42.92 J/m^2, respectively. Since the balloon could not maintain its orientation, the illumination angle of the sample changed with the balloon rotation during the flight, causing the light intensity value to fluctuate randomly. The low-illumination region is around 10^3 *Lx* representing the BIOSEP with its back to the Sun where the direct UV radiation for samples is negligible. Therefore, we estimated the direct exposure time of samples to be 5 hours 18 minutes. Accordingly, the estimated diffuse UV radiation dose received by samples during the direct exposure was ~2.42×10^4 J/m^2 (8.59 J/m^2 for VUV, 1.52×10^2 J/m^2 for UVC, 2.08×10^3 J/m^2 for UVB and 2.20×10^4 J/m^2 for UVA). According to the MODerate resolution atmospheric TRANsmission (MODTRAN) model [4], the direct total solar UV spectrum at an altitude of 23 km near Dachaidan was approximately two orders of magnitude higher than the diffuse radiation spectrum and was estimated to be ~10^6 J/m^2, mostly contributed from the significant enhancement in UVA. For the UVC band, the diffuse radiation dose was comparable to the direct solar radiation dose. For the UVB band, the direct solar

radiation dose was ~7.26×10^4 J/m^2, which was about 35 times higher than the diffuse radiation dose.

Activation and enumeration

After returning from near space, the sample chamber cells were wiped with 75% alcohol and disassembled under strictly sterile conditions. 2 ml of the LA2 medium were used to resuspend the freeze-dried MSR-1 samples. The suspensions were then 10-fold serially diluted to a final dilution factor of 1/100. A required volume of the suspensions was spread over the LA2 agar and incubated for 168 hours at 30°C. The number of survivors in each sample was estimated by colony-forming unit (CFU) enumeration, calculated as $C = N \times d / V$, where N is the average colony count, d is the dilution factor and V is the volume of the bacterial suspensions spread. Survival rates were determined as C_i / C_c, where C_i is the CFU in respective experimental groups and C_c is the CFU in the laboratory controls.

Transmission electron microscopy (TEM) analysis

Sterilized cell scrapers were used to gently collect the colonies from the culture plates and prevent defacing the agar. About 1 μL of bacterial colonies was diluted with Milli-Q water and deposited onto carbon-coated copper grids for TEM observation. Images of bacteria were captured using a JEOL JEM2100 TEM (Tokyo, Japan) operating at a 200-kV accelerating voltage. The number and crystal size of magnetosomes within MSR-1 were measured using ImageJ (v.1.50b) [5].

Rock magnetic measurement

Pure bacterial colonies collected from the culture plates were transferred into non-magnetic capsules, followed by the centrifugation at 12000 g for 1 minute and the air-drying in an anaerobic glove box to avoid possible oxidation. Hysteresis loop, backfield curve and first-order reversal curve (FORC) of each sample were determined using a PMC Micromag 3900 vibrating sample magnetometer (VSM, Princeton Measurements Corporation, Princeton, NJ, USA). The hysteresis loops were measured with a maximum field of 500 mT, a measurement step of 4.0 mT and an averaging time of 500 ms. The saturation magnetization (M_s), saturation remanence (M_{rs}), and coercivity (B_c) of the magnetic bacteria were obtained from hysteretic

measurements, and both M_s and M_{rs} were normalized to the maximum value of M_s. The B_{cr} value was retrieved from the backfield curve. For each sample, a total of 150 first-order reversal curves (FORCs) were determined with a saturation field of 1 T, a field step of 1.46 mT and an averaging time of 300 ms. The FORC diagrams were calculated using the FORCinel (v.3.06) software [6]. The smoothing factor of each FORC diagram was: $S_{c,0} = 4$, $S_{c,1} = 5$, $S_{b,0} = 4$, $S_{b,1} = 5$, and $\lambda_c = \lambda_b = 0.1$ [7]. The low-temperature measurements were conducted on one representative sample of each of the three groups using a SQUID MPMS XL-5 magnetic property measurement system (Quantum Design, San Diego, CA, USA). For zero-field cooled (ZFC) curve, after each sample was zero-field cooled from 300 K to 15 K, a saturation isothermal remanent magnetization (SIRM) was obtained at 15 K in a 2.5-T field before warming back to 300 K in a zero field. For field cooled (FC) curve, after each sample was cooled in a 2.5-T field from 300 K to 15 K, the sample was warmed from 15 K to 300 K in a zero field. For both ZFC and FC curves, the magnitude of SIRM was measured at 5 K intervals.

References

[1] Schüler D, Köhler M. The isolation of a new magnetic spirillum. Zentralbl Mikrobiol 1992; 147: 150-151.

[2] Heyen U, Schüler D. Growth and magnetosome formation by microaerophilic *Magnetospirillum* strains in an oxygen-controlled fermentor. Appl Microbiol Biotechnol 2003; 61: 536-544.

[3] Zhang Y, Zhang X, Jiang W, et al. Semicontinuous culture of *Magnetospirillum gryphiswaldense* MSR-1 cells in an autofermentor by nutrient-balanced and isosmotic feeding strategies. Appl Environ Microbiol 2011; 77: 5851-5856.

[4] Berk A, Conforti P, Kennett R, et al. MODTRAN6: a major upgrade of the MODTRAN radiative transfer code. 2014 6th Workshop on Hyperspectral Image and Signal Processing: Evolution in Remote Sensing (WHISPERS) 2014; 90880H.

[5] Schneider CA, Rasband WS, Eliceiri KW. NIH Image to ImageJ: 25 years of image analysis. Nat Methods 2012; 9: 671-675.

[6] Harrison RJ, Feinberg JM. FORCinel: An improved algorithm for calculating first-order reversal curve distributions using locally weighted regression smoothing. Geochem Geophys Geosyst 2008; 9: Q05016.

[7] Egli R. VARIFORC: An optimized protocol for calculating non-regular first-order reversal curve (FORC) diagrams. Glob Planet Change 2013; 110: 302-320.

Supplementary figures and tables

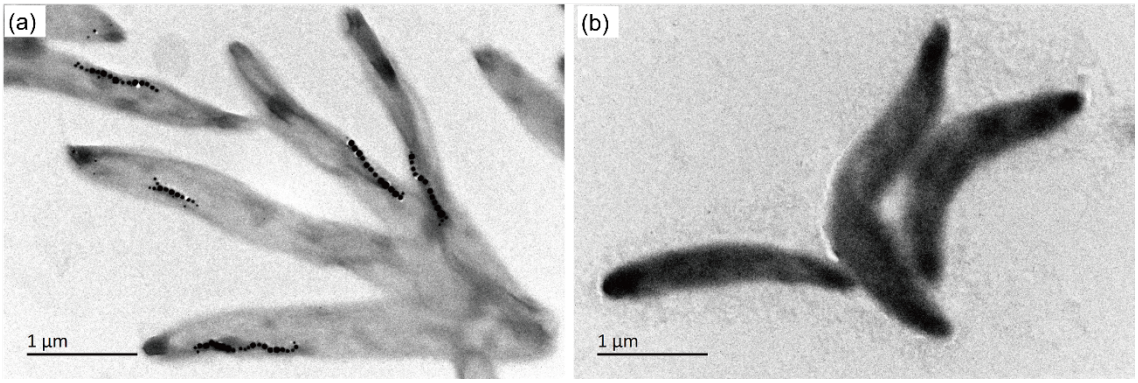

Figure S1. Two groups of *Magnetospirillum gryphiswaldense* strain MSR-1 (MSR-1) used in this study: (**a**) MSR-1(+) with intracellular magnetosomes and (**b**) MSR-1(-) without intracellular magnetosomes. The proportion of cells with magnetosomes accounted for about 85% of the total cells in MSR-1(+) group and less than 1% in MSR-1(-) group as revealed by TEM observation.

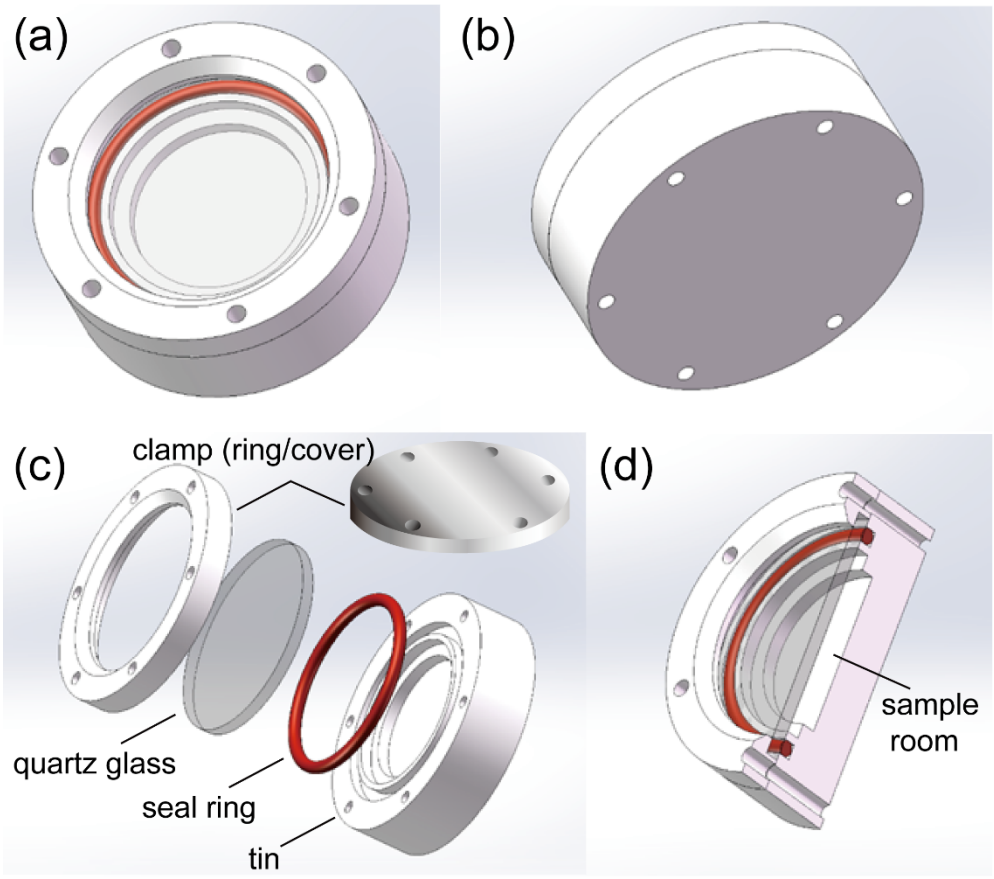

Figure S2. Schematic diagrams of sample chamber cells. (**a**) Front view and (**b**) rear view of a chamber cell. (**c**) Exploded view of a sample chamber cell illustrating the difference in clamps between the exposed group and the non-exposed group. (d) Cross-sectional view of a chamber cell.

Table S1. Numbers of *Magnetospirillum gryphiswaldense* strain MSR-1 (MSR-1) survived in near space-exposed group (NEG), near-space non-exposed group (NNG) and laboratory control group (LCG) as estimated by CFU enumeration.

	MSR-1(+) LCG (CFU)	MSR-1(+) NNG (CFU)	MSR-1(+) NEG (CFU)	MSR-1(-) LCG (CFU)	MSR-1(-) NNG (CFU)	MSR-1(-) NEG (CFU)
duplicate1	2.20×10^6	2.03×10^6	2.20×10^5	0.80×10^4	~4.00×10^3	0
duplicate2	1.90×10^6	~2.20×10^6	2.60×10^5	1.20×10^4	4.20×10^3	0
duplicate3	2.00×10^6	2.40×10^6	2.70×10^5	2.30×10^4	3.80×10^3	0
statistic	$2.03\pm0.12\times10^6$	$2.21\pm0.15\times10^6$	$2.50\pm0.22\times10^5$	$1.43\pm0.63\times10^4$	$4.00\pm0.16\times10^3$	0
rate	100.00%	108.69%	12.32%	100.00%	27.97%	0%

Table S2. The transmitted UVB radiation intensity (peaking at 297 nm with initial intensity of 4.1 W/m^2) through different layers of the MSR-1 cells.

	1 layer	2 layers	3 layers	4 layers	5 layers
MSR-1(+)	2.36 W/m^2	0.9 W/m^2	0.56 W/m^2	0.31 W/m^2	0.11 W/m^2
MSR-1(-)	2.35 W/m^2	0.89 W/m^2	0.59 W/m^2	0.47 W/m^2	0.29 W/m^2